ACS APPLIED MATERIALS & INTERFACES

Research Article

www.acsami.org

Fluorescent Organic Nanoparticles with Enhanced Fluorescence by Self-Aggregation and their Application to Cellular Imaging

Fu Tang, Chun Wang, Jinshan Wang, Xiaoyu Wang, and Lidong Li*

School of Materials Science and Engineering, University of Science and Technology Beijing, Beijing 100083, People's Republic of China

ABSTRACT: We report a simple strategy to prepare organic biocompatible fluorescent nanoparticles with enhanced fluorescence. A significant fluorescence enhancement was realized by designing a fluorescent small molecule, 4,4′-(2,7-bis[4-{1,2,2-triphenylvinyl}phenyl]-9*H*-fluorene-9,9-diyl)bis(*N*,*N*,*N*-trimethylbutan-1-aminum)bromide (TPEFN), with aggregation-induced emission enhancement (AIEE) effect. Nanoparticles of TPEFN can be formed through molecular self-aggregation by gradually increasing the water fraction in TPEFN mixed solution (methanol/water). Fluorescence enhancement by about 120-fold was observed after nanoparticle formation. By addition of the biomolecule adenosine triphosphate (ATP), larger nanoparticles of TPEFN are formed and further fluorescence enhancement can be achieved, yielding a total fluorescence enhancement of 420-fold compared with the TPEFN molecular solution. Both of these nanoparticles show very good biocompatibility. Ultrabright spots present in the confocal laser scanning microscopy image again proved the formation of nanoparticles. Positively charged side chains of TPEFN endow these nanoparticles cationic surfaces. The size of the prepared TPEFN nanoparticles and their cationic surface allow them to be rapidly internalized into cells. Cell viability assays prove that the TPEFN nanoparticles have high biocompatibility. These organic fluorescent nanoparticles show great promise for applications in cellular imaging or biotechnology.

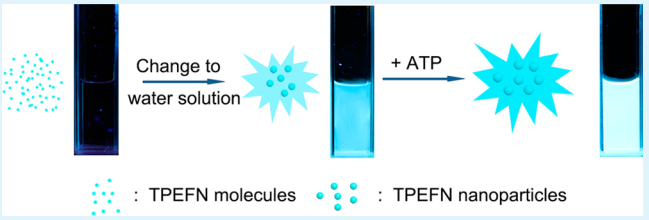

KEYWORDS: *fluorescence, nanoparticle, self-aggregation, enhanced fluorescence, cellular imaging, quenching*

INTRODUCTION

In recent years, fluorescent organic nanoparticles have attracted significant attention because of their unique optical and electrical properties. Compared with metal and inorganic nanoparticles, organic nanoparticles have more advantages, because organic compounds are cheaper than noble metals, they are easily modified with various functional groups, and they are simple to prepare.[1−13]

To fabricate fluorescent organic nanoparticles, one can choose different fluorescent materials, for example, fluorescent small molecules, oligomers, or fluorescent polymers.[14−18] For the fabrication of fluorescent organic nanoparticles, self-assembly is a useful technique, because it is a simple process applicable to various materials.[19−24] For example, by simply blending oppositely charged fluorescent molecules and coassembling reagents in a certain ratio, fluorescent organic nanoparticles are formed through molecular self-assembly via a range of interactions, such as electrostatic interactions, hydrogen bonding, hydrophobic interactions, and covalent coupling. Fluorescent organic nanoparticles can also be generated from self-assembly of fluorescent molecules when there is a significant change in solvent polarity. Nanoparticles can be used for fluorescence imaging of live cells.[18,25−28] However, aggregation of fluorescent molecules in nanoparticles often results in decreased fluorescence or poor photochemical stability of the nanoparticles, primarily as a result of self-quenching.[29−31]

Recently, the novel phenomenon of aggregation-induced emission enhancement (AIEE) has been discovered that may result from a decrease of fluorescence quenching at high fluorophore concentrations.[32,33] AIEE occurs when fluorescent materials emit strongly in their aggregated state or solid state but give very weak emission in the solution state. This phenomenon was usually observed for molecules that contain rotor structures (such as silole and tetraphenylethene (TPE)). Simply attaching these structures to various fluorescent molecules can effectively transform them into AIEE molecules.[34−37] This approach can be employed to design and fabricate AIEE fluorescent materials with specific emission wavelengths and open new routes to fluorescent nanoparticles.

In this work, we report a simple strategy to prepare a strongly fluorescent organic nanoparticle through the self-assembly of the fluorescent small molecule 4,4′-(2,7-bis[4-{1,2,2-triphenylvinyl}phenyl]-9*H*-fluorene-9,9-diyl)bis(*N*,*N*,*N*-trimethylbutan-1-aminum)bromide (TPEFN). The hydrophilic positively charged side chains and the hydrophobic backbone of TPEFN facilitate nanoparticle formation. The as-prepared TPEFN is nonemissive in methanol (MeOH) solution but emits strongly when TPEFN nanoparticles are formed owing to the addition of water as a poor solvent. Interestingly, such

Received: August 26, 2014
Accepted: October 2, 2014
Published: October 2, 2014

TPEFN nanoparticles can be adjusted by adding the biomolecule adenosine triphosphate (ATP), which results in larger nanoparticles and a significant additional fluorescence enhancement. This makes TPEFN nanoparticles an excellent material for fluorescence imaging. Furthermore, the TPEFN nanoparticles show very good biocompatibility. The positive charge of the TPEFN side chains allows them to be rapidly internalized into cells. Cell viability assay proved these nanoparticles show very little cytotoxicity to cells. These properties make the as-prepared TPEFN nanoparticle a good material for cell imaging.

EXPERIMENTAL SECTION

Materials and Measurements. The compound 2,2′-(9,9-bis[4-bromobutyl]-9*H*-fluorene-2,7-diyl)bis(4,4,5,5-tetramethyl-1,3,2-dioxaborolane) (**1**) was synthesized according to the literature.[38] 1-(4-Bromophenyl)-1,2,2-triphenylethylene was purchased from J&K Chemical Co. Trimethylamine solution (31−35 wt % in ethanol) was purchased from Sigma-Aldrich. Other reagents used in the experiments were purchased from J&K Chemical or Sigma-Aldrich and were used without further purification, unless otherwise noted. Distilled water was used. Ultraviolet−visible (UV−vis) absorption spectra were collected on a Hitachi U-3900H spectrophotometer. Photoluminescence (PL) emission spectra were measured on a Hitachi F-7000 fluorescence spectrophotometer. The ^{1}H NMR and ^{13}C NMR spectra were recorded on a 400 MHz AC Bruker spectrometer. Chemical shifts are reported in parts per million (ppm) relative to an internal standard, either tetramethylsilane ($Si[CH_3]_4$ = 0.00 ppm) or residual solvent peaks ($CDCl_3$ = 7.26 ppm, DMSO-d_6 = 2.50 ppm, CD_3OD = 3.31 ppm). ^{1}H NMR coupling constants (J) are reported in Hertz (Hz) and multiplicity is indicated as follows: s (singlet), d (doublet), t (triplet), q (quartet), m (multiplet), br s (broad singlet), br d (broad doublet), dd (doublet of doublet), dt (doublet of triplet), dq (doublet of quartet), and tq (triplet of quartet). Mass spectra were obtained using a Bruker Daltonics BIFLEX III matrix-assisted laser desorption/ionization time-of-flight (MALDI-TOF) analyzer in MALDI mode. The ζ-potential and size distributions of the nanoparticles in aqueous solution were measured by dynamic light scattering with a Malvern Zetasizer Nano ZS90 at room temperature. The fluorescence image of TPEFN nanoparticles was recorded using an Olympus FV1000-IX81 confocal laser scanning biological microscope, with 330−380 nm excitation by a 100 W mercury lamp light source. Fluorescence images of cells were recorded using an Olympus 1X71 fluorescence microscope with 405 nm excitation.

The morphology of the nanoparticles was observed using high-resolution field emission scanning electron microscopy (HRSEM, JEOL JSM-7401F, accelerating voltage: 3.0 kV). The samples were prepared by adding 5 μL of TPEFN MeOH solution (2 mM) into 2 mL of water followed by no ATP addition or 5 μL of ATP (2 mM) solution, and then a droplet of the mixture was placed on 5 × 5 mm silicon wafer. After the samples dried at room temperature, they were coated with Pt (40 s) to facilitate the observation. Photographs were taken with a Canon EOS 650D under 365 nm UV light.

Synthesis of 9,9-Bis(4-bromobutyl)-2,7-bis(4-(1,2,2-triphenylvinyl)phenyl)-9*H*-fluorene (TPEF). Compound **1** (0.68 g, 1 mM) and 1-(4-bromophenyl)-1,2,2-triphenylethylene (0.92 g, 2.2 mM) were dissolved into 20 mL of toluene, and then 5 mL of 2.0 M potassium carbonate solution was added. After the solution was degassed with nitrogen for 30 min, 12 mg of catalyst $Pd(PPh_3)_4$ was added. The mixture was stirred at 90 °C for 36 h under nitrogen atmosphere. The solution was cooled and extracted with $CHCl_3$ after adding 30 mL of water. The organic layer was combined and dried over anhydrous sodium sulfate. The solvent was removed and the crude product was obtained by column chromatography, yielding a yellow-green solid (yield 68%), which was used directly for the next step. ^{1}H NMR (400 MHz, $CDCl_3$): δ 7.69 (d, J = 7.7 Hz, 2H), 7.53 (d, J = 8.0 Hz, 2H), 7.49 (d, J = 5.8 Hz, 2H), 7.41 (d, J = 8.4 Hz, 4H), 7.15−7.04 (m, 30H), 7.03 (dd, J = 5.2, 2.5 Hz, 4H), 3.13 (t, J = 6.9 Hz, 4H), 2.09−1.91 (m, 6H), 1.59 (dd, J = 12.5, 5.3 Hz, 6H). ^{13}C NMR (101 MHz, $CDCl_3$): δ 150.47, 143.79, 142.81, 141.15, 140.55, 139.97, 139.80, 139.04, 131.86, 131.43, 131.39, 131.36, 127.82, 127.71, 127.64, 126.51, 126.22, 120.82, 120.03, 54.81, 39.24, 32.82, 31.85, 29.92, 22.15, 13.96. MS (MALDI-TOF) m/z: M^+ calcd: 1096.3. Found: 1096.3.

Synthesis of 4,4′-(2,7-Bis(4-(1,2,2-triphenylvinyl)phenyl)-9*H*-fluorene-9,9-diyl)bis(*N*,*N*,*N*- trimethylbutan-1-aminum)-bromide (TPEFN). 100 mg of TPEF was dissolved into 50 mL of chloroform. A 31−35 wt % trimethylamine−ethanol solution (3 mL) was then added. The mixture was stirred for 72 h at room temperature. The solvents were removed by evaporation under vacuum and TPEFN was obtained after drying in a vacuum. ^{1}H NMR (400 MHz, CH_3OD): δ 7.78 (d, J = 7.9 Hz, 2H), 7.69 (s, 2H), 7.59 (d, J = 7.7 Hz, 2H), 7.47 (d, J = 8.0 Hz, 4H), 7.12 (dd, J = 17.1, 7.4 Hz, 27H), 7.06−6.98 (m, 7H), 3.06−2.87 (m, 22H), 2.33−2.20 (m, 4H), 1.54 (s, 2H), 1.29 (d, J = 10.8 Hz, 4H). ^{13}C NMR (101 MHz, CD_3OD): δ 150.34, 143.77, 143.65, 142.94, 141.34, 140.55, 140.16, 139.91, 138.87, 131.60, 131.01, 130.99, 130.93, 127.50, 127.41, 127.35, 126.29, 126.23, 126.18, 125.93, 125.80, 120.89, 120.00, 66.04, 54.92, 52.03, 39.17, 22.65, 20.67. MS (MALDI-TOF) m/z: M^+ calcd: 1054.62. Found: $[M - CH_3]^+$ = 1039.6.

Aggregation Induced Emission Enhancement Assay. Solutions of TPEFN in MeOH/H_2O mixtures were prepared by adding the stock solution of TPEFN (5 μL, 2 mM in MeOH) into 2 mL of MeOH/H_2O mixture with various water fractions (MeOH/H_2O = 100% MeOH, 90%/10%, 80%/20%, 70%/30%, 60%/40%, 50%/50%, 40%/60%, 30%/70%, 20%/80%, 10%/90%, 5%/95%, 1%/99%, 100% H_2O in volume). UV−vis absorption spectra were measured immediately using a Hitachi U3900H spectrophotometer. Fluorescence spectra were obtained after the UV−vis observation by using a Hitachi F-7000 fluorescence spectrometer equipped with a xenon lamp excitation source at room temperature. The excitation wavelength was 354 nm. The fluorescence photographs were taken under a UV lamp with 365 nm excitation.

Cytotoxicity Assay by MTT Method. A549 lung cancer cells were seeded into 96-well plates and maintained overnight in Dulbecco's modified Eagle's medium (DMEM) containing 10% fetal bovine serum (FBS) (v/v), and then treated using various concentrations of TPEFN nanoparticles (0−15 μM) at 37 °C for 24 h. The concentration of TPEFN nanoparticles was determined using the concentration of TPEFN molecules. After the medium was poured out, 100 μL of freshly prepared 3-(4,5-dimethylthiazol-2-yl)-2,5-diphenyltetrazolium bromide (MTT, 1 mg/mL in phosphate buffered saline [PBS]) was added to each well and the wells were incubated for 4 h. The supernatant was removed, and the cells were lysed by adding 100 μL of DMSO per well. The plate was gently shaken for 5 min, and then the absorbance of purple formazan at 520 nm was monitored using a Spectra MAX 340PC plate reader.

Cell Imaging Assay. A549 cells were grown in DMEM medium containing 10% FBS, and 100 000 cells were then seeded on 35 × 35 mm culture plates and the plates were incubated at 37 °C in a 5% CO_2 humidified atmosphere for 24 h. TPEFN nanoparticles were added to 1 mL of medium containing A549 cells in a 35 × 35 mm plate (final concentration [TPEFN] = 5 μM). After incubation at 37 °C for 4 h, the medium was removed, and the cells were washed twice using PBS buffer (pH 7.4). Then the specimens were observed using an oil immersion lens (100× magnification, NA 1.4) with an Olympus FV1000-IX81 confocal laser scanning microscope, using a DM405/488 dichroic mirror capturing within a bandwidth of 460−560 nm for the 405 scan.

RESULT AND DISCUSSION

Synthesis and Characterization of TPEFN. The AIEE active TPEFN molecule was obtained by reaction of two tetraphenylethene (TPE) groups to a fluorene unit. Fluorene was chosen for its planar and rigid aromatic ring structure, which ensures a high degree of conjugation, and its synthetic versatility at the benzylic 9-position and aromatic 2,7-positions

Scheme 1. Synthesis Route of TPEFN Molecules

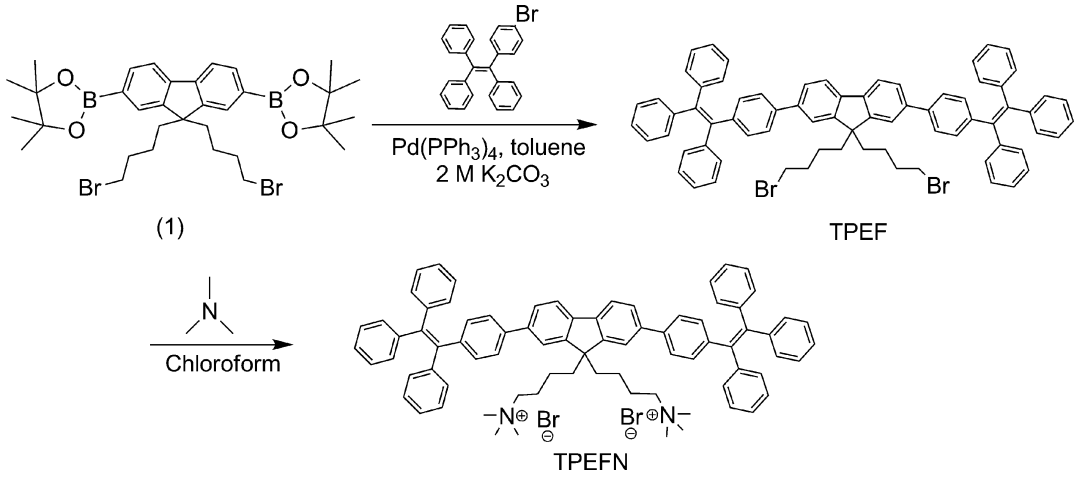

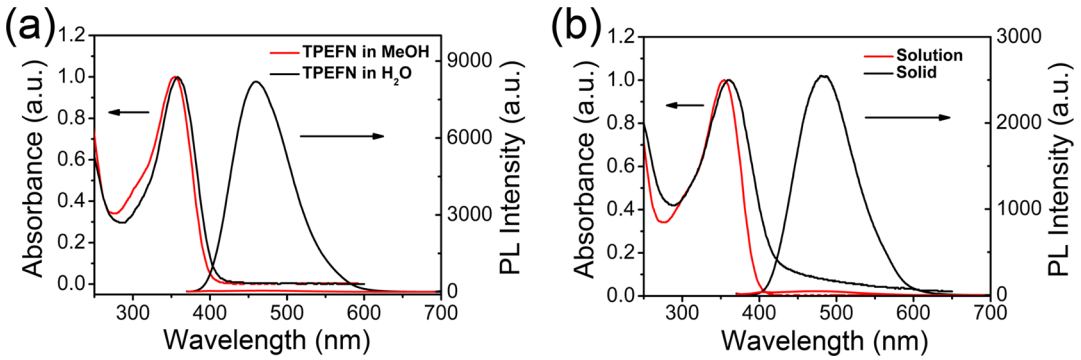

Figure 1. (a) Absorption and PL spectra of TPEFN in MeOH and water, and (b) comparison of the absorption and PL intensity of TPEFN in MeOH solution and solid film. TPEFN concentrations in MeOH and water were 5 μM, and the absorbance was normalized.

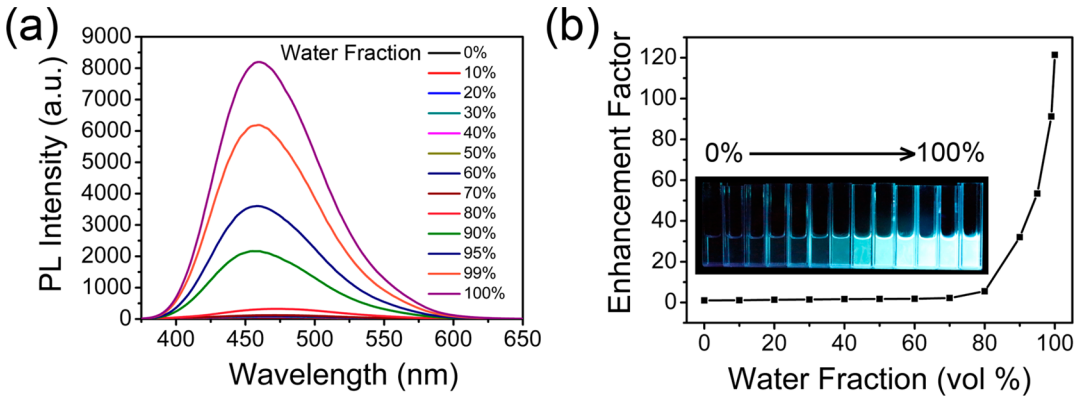

Figure 2. (a) PL spectra of TPEFN in MeOH/H_2O mixtures with different water fractions. (b) Plots of relative emission intensity enhancement factors versus aqueous mixture content with different water fractions. TPEFN concentration: 5 μM. Excitation wavelength: 354 nm. Inset: photograph of TPEFN in MeOH/H_2O mixtures with different water fractions from 0% to 100% (in vol %) at 365 nm UV irradiation.

facilitates further design and synthesis.[35,36,39] Positively charged TPEFN molecules can be synthesized by simply modifying the fluorene side chains with quaternary ammonium. The rotation of aromatic rotors of TPE groups annihilates the excitons in a nonradiative manner when TPEFN was in the solution state. But when aggregates of TPEFN formed, the aggregated state restricts the rotation behavior and thus populates the radiative decay of the excitons, resulting in enhanced emission.[40] The chemical structure and synthesis procedures of TPEFN is shown in Scheme 1. TPEF was first obtained via the Suzuki cross-coupling reaction of 1-(4-bromophenyl)-1,2,2-triphenylethylene and 2,2′-(9,9-bis[4-bromobutyl]-9*H*-fluorene-2,7-diyl)bis(4,4,5,5-tetramethyl-1,3,2-dioxaborolane) (compound **1**). The intermediate compound **1** was prepared according to the reported procedures.[38] After dissolution in chloroform, the TPEF was treated with 31−35% trimethylamine solution at room temperature for 72 h, and positively charged TPEFN was obtained after removal of the solvent. It can be readily dissolved in organic solvents, such as methanol, acetonitrile, and dimethyl sulfoxide, but is nearly insoluble in water. In our work, the TPEFN was dissolved in MeOH at a concentration of 2 mM.

The photophysical properties of TPEFN were investigated both in MeOH and water. Five microliters of TPEFN in MeOH solution was added to 2 mL of MeOH or water, respectively. As seen from Figure 1a, the UV−vis absorption spectrum of TPEFN in MeOH shows maximum absorption at 354 nm, and there is a red shift of about 4 nm, if water is used as the dispersant, which suggests *J*-aggregate formation.[37,41] TPEFN shows nearly no emission in dilute MeOH solution (Figure 1a), which may be caused by active intramolecular rotations of the phenyl rings from the TPE end groups. If water is used as the main solvent, TPEFN emits strongly, which suggests a restriction of the intramolecular rotation and thus blocks the nonradiative decay channels and facilitates radiative transitions.[31,42] The solid powder of TPEFN appears slightly yellow-green. TPEFN in solid film (prepared by spin-coating 2 mM/0.3 mL × 3 TPEFN MeOH solution onto a quartz substrate) also shows a red shifted absorption and emits strongly when excited at its maximum absorption wavelength as compared with its diluted MeOH solution state (Figure 1b). These results suggest that TPEFN is a potent AIEE molecule.

Aggregation Induced Emission Enhancement Assay. To further study the AIEE behavior of the TPEFN molecules, their emission spectra were measured in MeOH/H_2O mixtures. As TPEFN is nearly insoluble in water, it should self-assemble into aggregates, if significant quantities of water are added to the MeOH stock solution of TPEFN. Figure 2a shows the emission spectra of TPEFN in the MeOH/H_2O mixture with various water fractions. From the spectra, we can see that the PL intensity of TPEFN solution increases as the water fraction in the MeOH/H_2O mixture increases. When the water content is below 60% (vol %), the emission intensity of TPEFN solution is very weak and varies only slightly. However, it starts to increase and continues to increase strongly as larger amounts of water are added. This trend can also be observed from the fluorescence photograph (Figure 2b inset) of TPEFN in MeOH/H_2O mixtures (with various water fractions) under a 365 nm UV excitation. The TPEFN shows almost no fluorescence emission when the water content is below 60%. Blue fluorescence is observed as the water content increases and reaches the brightest state as the volume percentage of water rises to nearly 100%. Figure 2b gives the relative emission enhancement factors of TPEFN in MeOH/H_2O mixtures with various water fractions. The enhancement factors were defined as the ratios of integral area of the PL spectra of TPEFN in MeOH/H_2O mixtures with different water fractions to that of in pure MeOH. The concentration of TPEFN in each MeOH/H_2O mixture was maintained at 5 μM. Maximum fluorescence enhancement of about 120-fold is obtained when TPEFN is in a 100% water solution. These results demonstrate that TPEFN is a typical AIEE-active molecule.

As the TPEFN aggregates are homogeneous in all the solutions without precipitates, and remain stable for weeks at 4 °C, we expect that the aggregates are nanosized. To prove this, TPEFN in a 100% water solution (TPEFN concentration: 5 μM) was studied by SEM (Figure 3a). From the SEM image we can clearly see that the aggregates formed by TPEFN are nanoparticles that are approximately spherically shaped. Most of the nanoparticles possess an average diameter of around 50 nm with a small fraction of particles with diameters above 100 nm. The nanoparticles disperse very well, with no obvious aggregation seen from the observation scope. We suppose that the positively charged surface of the nanoparticles is the key to keeping the colloidal solution stable. As the TPEFN molecular

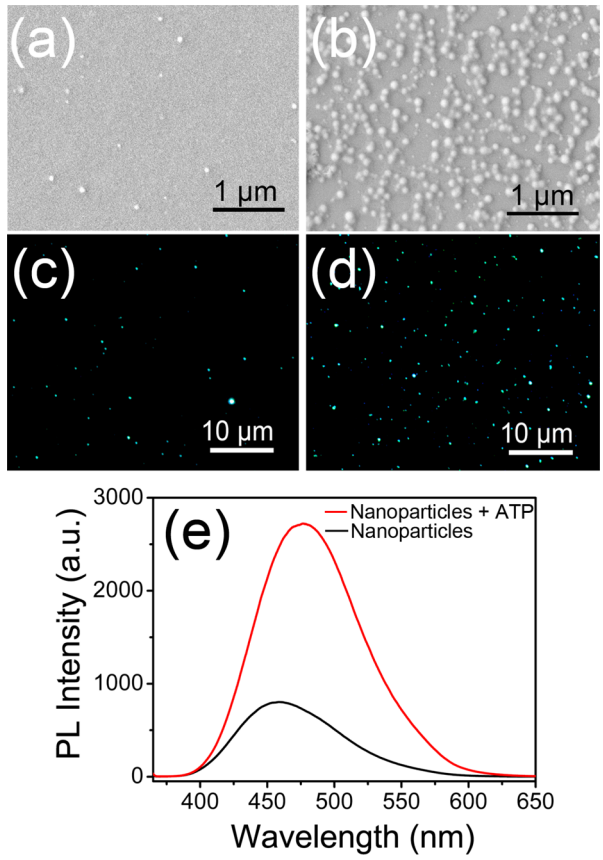

Figure 3. SEM (top row) and CLSM (bottom row) micrographs of TPEFN nanoparticles before (a, c) and after (b, d) addition of ATP. (e) PL spectra of TPEFN nanoparticle solution before and after the addition of ATP. (TPEFN and ATP concentration are 5 μM).

backbone is hydrophobic, and the quaternary ammonium modified side chains of the fluorene units are positively charged and hydrophilic, in its poor solvent water, TPEFN molecules may precipitate from the solubility change and aggregate to form nanoparticles in which hydrophobic moieties of TPEFN tends to imbedded inside leading more hydrophilic moieties gather at the surface of nanoparticles. In accordance with this the ζ potential of the nanoparticles in the aqueous solution is positive (39.6 ± 2.3 mV). We can conclude that it is the special amphiphilic structure of the TPEFN molecule, that facilitates the nanoparticle formation, and the electrostatic repulsion between the TPEFN nanoparticles is the main reason that the nanoparticles remain in a stable colloidal state.

Given the small number of TPEFN nanoparticles formed in aqueous solution, we postulate a large quantity of TPEFN molecules still exist in a free state that have not aggregated. The biomolecule ATP was used to adjust the TPEFN nanoparticle formation. We choose ATP because it has three sequential phosphate groups that are negatively charged at neutral pH. As the TPEFN molecule is positively charged, the electrostatic interaction may result in rapid molecular self-assembly, allowing more TPEFN nanoparticles to be formed simultaneously. The SEM analysis (Figure 3b) proved our assumption. As we can see from Figure 3b, after the addition of ATP, a great number of TPEFN nanoparticles appeared in the observation area, which shows a sharp contrast to the SEM image of Figure 3a, in which much fewer TPEFN nanoparticles can be observed without the addition of ATP.

Interestingly, in the absence of ATP, the average size of TPEFN nanoparticles was around 50 nm, but when ATP was added, larger nanoparticles of around 100 nm could be clearly observed. Confocal laser scanning microscopy (CLSM) images of TPEFN colloidal solution without (Figure 3c) and with (Figure 3d) addition of ATP gives directly visual images of the TPEFN fluorescent nanoparticles. More cyanic particles with brighter fluorescence can be observed after ATP addition. The fluorescent nanoparticles are of good dispersibility, as very little nanoparticle aggregation can be observed. PL spectra of TPEFN before and after ATP addition (Figure 3e) show that the fluorescence is considerably enhanced after addition of ATP as compared with the PL intensity of TPEFN nanoparticles in 100% water solution. The fluorescence intensity enhancement factor was an additional 3.5-fold, which results in about 420-fold fluorescence enhancement of TPEFN compared to 100% MeOH solution. A red shift of about 25 nm can be observed from the PL spectrum after ATP addition. This may be due to a much more ordered intermolecular packing as the aggregation behavior of TPEFN molecules could be tuned by the addition of ATP.

In this work, fluorescent organic nanoparticles can be obtained by self-assembly via electrostatic interaction by simply mixing oppositely charged molecules in a certain ratio. If TPEFN molecules dissolved in organic solvent are first added to an excess of their poor solvent (water), TPEFN nanoparticles are formed owing to the precipitation of TPEFN molecules from the good solvent. However, there should be some molecules that remain dissolved as the TPEFN molecule possesses hydrophilic cationic side chains that may have very low solubility in aqueous solution. With the addition of ATP, the electrostatic interactions between the quaternary ammonium modified side chain of TPEFN molecules and the triphosphate moiety of ATP facilitate the assembly of TPEFN molecules. That is, more TPEFN molecules participate in the assembly through ATP linkage. Thus, larger and many more TPEFN nanoparticles are formed. The hydrophobicity of the adenine moiety of ATP also facilitates the nanoparticle formation. Compared with TPEFN nanoparticles formed without ATP, the newly formed nanoparticles are more tightly packed owing to the electrostatic interaction, and the adenine moiety of ATP and the backbone of TPEFN molecules can lead to collective $\pi-\pi$ stacking, which restricts the intramolecular rotations of the phenyl rings in TPE, and thus enhances the fluorescence of TPEFN molecules to a much higher degree.

Cellular Internalization Assay and Cell Viability Assay. To demonstrate the applications of ultrabright TPEFN nanoparticles for biological imaging, an important question needs to be answered, could these nanoparticles be taken up by cells? Motivated by this question, we incubated A549 lung cancer cells at 37 °C for 4 h with TPEFN nanoparticles and with TPEFN nanoparticles adjusted by ATP addition. Figure 4 shows confocal microscopy images of the A549 cells taken after incubation for 4 h (Figure 4a for TPEFN nanoparticles, Figure 4b for TPEFN nanoparticles adjusted by ATP). Both nanoparticles showed very good cellular uptake as bright cyanic fluorescence was observed in the cytoplasm of the A549 cells from the CLSM images. A stronger fluorescence signal was observed from the A549 cells incubated with TPEFN nanoparticles that had been adjusted by ATP. These results again proved the additional fluorescence enhancement effect by ATP addition and showed the high potential of these TPEFN nanoparticles for applications in live cell imaging.

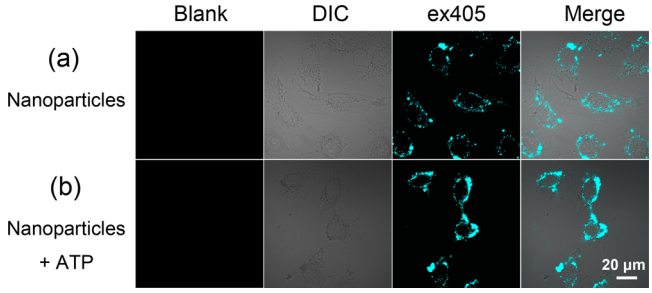

Figure 4. Confocal laser scanning microscopy images of A549 cells, which were either incubated with TPEFN nanoparticles (a) or TPEFN nanoparticles adjusted by ATP (b) for 4 h at 37 °C. The fluorescence images were obtained using a 405 nm laser. The scale bar represents 20 μm. The concentration of TPEFN molecules was 5 μM.

For biological applications, it is important that the fluorescent nanoparticles have good biocompatibility with low toxicity. We investigated the cytotoxicity of both TPEFN nanoparticles by using a MTT cell-viability assay. The absorbance of MTT at 490 nm is dependent on the degree of activation of the cells. The cell viability was thus expressed by the ratio of absorbance of the cells incubated with various concentrations of TPEFN nanoparticles to that of the cells incubated with culture medium only. As shown in Figure 5, the

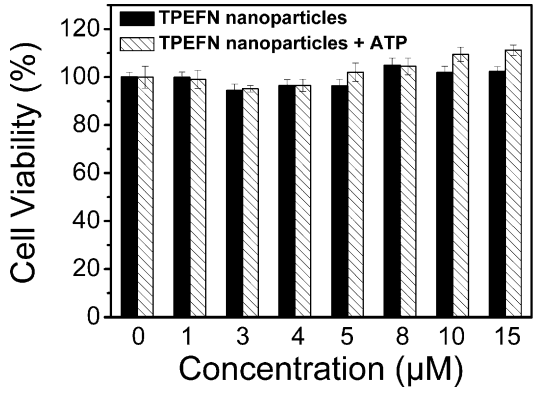

Figure 5. Cell viability results after incubation of A549 cells with various concentrations of TPEFN nanoparticles. The cell viability percentage is calculated relative to that of cells without adding TPEFN nanoparticles, which is defined as a viability of 100%.

cell viability of both nanoparticles decreases very little after 24 h incubation of A549 cells with various concentrations of TPEFN nanoparticles ([TPEFN] = 0–15 μM). The cell viability ratios are nearly 100% in the testing range, which indicates that the TPEFN molecules have little effect on the cellular activity. Moreover, as ATP is a known biomolecule that has good biocompatibility, the cytocompatibility of TPEFN nanoparticles was slightly enhanced after the addition of ATP. The good biocompatibility makes the TPEFN nanoparticles suitable for live cell imaging.

CONCLUSION

In this work, we report a simple strategy to prepare organic biocompatible fluorescent nanoparticles with enhanced fluorescence. Significant fluorescence enhancement was realized by designing a fluorescent small molecule (TPEFN) with typical aggregation-induced emission enhancement (AIEE) effect. TPEFN nanoparticles could be obtained by gradually increasing

the water fraction in the TPEFN mixed solution, which leads to about 120-fold fluorescence enhancement. The biomolecule ATP can be used to adjust the nanoparticle formation, and results in an additional fluorescence enhancement as high as 420-fold. Ultrabright spots present in the confocal laser scanning microscopy images prove the nanoparticle formation. Positively charged side chains of TPEFN endow its nanoparticles with a cationic surface. The size and cationic charge of the TPEFN nanoparticles allow them to be rapidly internalized into cells. Cell viability assays prove that the TPEFN nanoparticles have high biocompatibility. All properties presented here show that these bright fluorescent organic nanoparticles are a novel and efficient material for cellular imaging or biotechnology.

AUTHOR INFORMATION

Corresponding Author

*L. L. E-mail: lidong@mater.ustb.edu.cn.

Notes

The authors declare no competing financial interest.

ACKNOWLEDGMENTS

This work was supported by the National Natural Science Foundation of China (51403018, 51373022), Research Fund for the Doctoral Program of Higher Education of China (20130006110007), the Fundamental Research Funds for the Central Universities (FRF-SD-12-005B), Beijing Municipal Science and Technology Commission (Z131100005213008) and the Program for Chang Jiang Scholars and Innovative Research Team in University. The authors thank Prof. Helmuth Möhwald for his helpful suggestions and discussions in this research. The authors thank Dr. Libin Liu for giving support for the cellular experiments.

REFERENCES

(1) Xu, X.; Chen, S.; Li, L.; Yu, G.; Di, C.; Liu, Y. Photophysical Properties of Polyphenylphenyl Compounds in Aqueous Solutions and Application of Their Nanoparticles for Nucleobase Sensing. *J. Mater. Chem.* **2008**, *18*, 2555−2561.

(2) Zheng, C.; Xu, X.; He, F.; Li, L.; Wu, B.; Yu, G.; Liu, Y. Preparation of High-Quality Organic Semiconductor Nanoparticle Films by Solvent-Evaporation-Induced Self-Assembly. *Langmuir* **2010**, *26*, 16730−16736.

(3) Wang, J.; Xu, X.; Shi, L.; Li, L. Fluorescent Organic Nanoparticles Based on Branched Small Molecule: Preparation and Ion Detection in Lithium-Ion Battery. *ACS Appl. Mater. Interfaces* **2013**, *5*, 3392−3400.

(4) Wang, X.; He, F.; Li, L.; Wang, H.; Yan, R.; Li, L. Conjugated Oligomer-based Fluorescent Nanoparticles as Functional Nanocarriers for Nucleic Acids Delivery. *ACS Appl. Mater. Interfaces* **2013**, *5*, 5700−5708.

(5) Wang, F.; Han, M.-Y.; Mya, K. Y.; Wang, Y.; Lai, Y.-H. Aggregation-Driven Growth of Size-Tunable Organic Nanoparticles Using Electronically Altered Conjugated Polymers. *J. Am. Chem. Soc.* **2005**, *127*, 10350−10355.

(6) Han, M.; Hara, M. Intense Fluorescence from Light-Driven Self-Assembled Aggregates of Nonionic Azobenzene Derivative. *J. Am. Chem. Soc.* **2005**, *127*, 10951−10955.

(7) Xiao, D.; Xi, L.; Yang, W.; Fu, H.; Shuai, Z.; Fang, Y.; Yao, J. Size-Tunable Emission from 1,3-Diphenyl-5-(2-anthryl)-2-pyrazoline Nanoparticles. *J. Am. Chem. Soc.* **2003**, *125*, 6740−6745.

(8) Zhu, L.; Yang, C.; Qin, J. An Aggregation-Induced Blue Shift of Emission and the Self-Assembly of Nanoparticles from a Novel Amphiphilic Oligofluorene. *Chem. Commun.* **2008**, 6303−6305.

(9) Vijayakumar, C.; Sugiyasu, K.; Takeuchi, M. Oligofluorene-based Electrophoretic Nanoparticles in Aqueous Medium as a Donor Scaffold for Fluorescence Resonance Energy Transfer and White-Light Emission. *Chem. Sci.* **2011**, *2*, 291−294.

(10) Koizumi, Y.; Seki, S.; Tsukuda, S.; Sakamoto, S.; Tagawa, S. Self-Condensed Nanoparticles of Oligofluorenes with Water-Soluble Side Chains. *J. Am. Chem. Soc.* **2006**, *128*, 9036−9037.

(11) Petkau, K.; Kaeser, A.; Fischer, I.; Brunsveld, L.; Schenning, A. P. H. J. Pre- and Postfunctionalized Self-Assembled π-Conjugated Fluorescent Organic Nanoparticles for Dual Targeting. *J. Am. Chem. Soc.* **2011**, *133*, 17063−17071.

(12) Tseng, K.-P.; Fang, F.-C.; Shyue, J.-J.; Wong, K.-T.; Raffy, G.; Guerzo, A. D.; Bassani, D. M. Spontaneous Generation of Highly Emissive RGB Organic Nanospheres. *Angew. Chem., Int. Ed.* **2011**, *50*, 7032−7036.

(13) Palacios, R. E.; Fan, F.-R. F.; Grey, J. K.; Suk, J.; Bard, A. J.; Barbara, P. F. Charging and Discharging of Single Conjugated-Polymer Nanoparticles. *Nat. Mater.* **2007**, *6*, 680−685.

(14) Feng, X.; Tang, Y.; Duan, X.; Liu, L.; Wang, S. Lipid-Modified Conjugated Polymer Nanoparticles for Cell Imaging and Transfection. *J. Mater. Chem.* **2010**, *20*, 1312−1316.

(15) Li, K.; Liu, B. Polymer-Encapsulated Organic Nanoparticles for Fluorescence and Photoacoustic Imaging. *Chem. Soc. Rev.* **2014**, *43*, 6570−6597.

(16) Yuan, H.; Liu, Z.; Liu, L.; Lv, F.; Wang, Y.; Wang, S. Cationic Conjugated Polymers for Discrimination of Microbial Pathogens. *Adv. Mater.* **2014**, *26*, 4333−4338.

(17) Li, L.; Shen, X.; Xu, Q.-H.; Yao, S. Q. A Switchable Two-Photon Membrane Tracer Capable of Imaging Membrane-Associated Protein Tyrosine Phosphatase Activities. *Angew. Chem., Int. Ed.* **2013**, *52*, 424−428.

(18) Feng, L.; Zhu, C.; Yuan, H.; Liu, L.; Lv, F.; Wang, S. Conjugated Polymer Nanoparticles: Preparation, Properties, Functionalization and Biological Applications. *Chem. Soc. Rev.* **2013**, *42*, 6620−6633.

(19) Decher, G. Fuzzy Nanoassemblies: Toward Layered Polymeric Multicomposites. *Science* **1997**, *277*, 1232−1237.

(20) Donath, E.; Sukhorukov, G. B.; Caruso, F.; Davis, S. A.; Möhwald, H. Novel Hollow Polymer Shells by Colloid-Templated Assembly of Polyelectrolytes. *Angew. Chem., Int. Ed.* **1998**, *37*, 2201−2205.

(21) Sukhorukov, G. B.; Antipov, A. A.; Voigt, A.; Donath, E.; Möhwald, H. pH-Controlled Macromolecule Encapsulation in and Release from Polyelectrolyte Multilayer Nanocapsules. *Macromol. Rapid Commun.* **2001**, *22*, 44−46.

(22) Skirtach, A. G.; Yashchenok, A. M.; Möhwald, H. Encapsulation, Release and Applications of LbL Polyelectrolyte Multilayer Capsules. *Chem. Commun.* **2011**, *47*, 12736−12746.

(23) Li, G. L.; Möhwald, H.; Shchukin, D. G. Precipitation Polymerization for Fabrication of Complex Core−Shell Hybrid Particles and Hollow Structures. *Chem. Soc. Rev.* **2013**, *42*, 3628−3646.

(24) Yan, Y.; Björnmalm, M.; Caruso, F. Assembly of Layer-by-Layer Particles and Their Interactions with Biological Systems. *Chem. Mater.* **2014**, *26*, 452−460.

(25) Xing, C.; Xu, Q.; Tang, H.; Liu, L.; Wang, S. Conjugated Polymer/Porphyrin Complexes for Efficient Energy Transfer and Improving Light-Activated Antibacterial Activity. *J. Am. Chem. Soc.* **2009**, *131*, 13117−13124.

(26) Tang, F.; He, F.; Cheng, H.; Li, L. Self-Assembly of Conjugated Polymer-Ag@SiO_2 Hybrid Fluorescent Nanoparticles for Application to Cellular Imaging. *Langmuir* **2010**, *26*, 11774−11778.

(27) Tang, F.; Ma, N.; Wang, X.; He, F.; Li, L. Hybrid Conjugated Polymer-Ag@PNIPAM Fluorescent Nanoparticles with Metal-Enhanced Fluorescence. *J. Mater. Chem.* **2011**, *21*, 16943−16948.

(28) Cui, Q.; He, F.; Wang, X.; Xia, B.; Li, L. Gold Nanoflower@Gelatin Core−Shell Nanoparticles Loaded with Conjugated Polymer Applied for Cellular Imaging. *ACS Appl. Mater. Interfaces* **2013**, *5*, 213−219.

(29) Birks, J. B. Excimers and Exciplexs. *Nature* **1967**, *214*, 1187−1190.

(30) Davis, R.; Kumar, N. S. S.; Abraham, S.; Suresh, C. H.; Rath, N. P.; Tamaoki, N.; Das, S. Molecular Packing and Solid-State

Fluorescence of Alkoxy-Cyano Substituted Diphenylbutadienes: Structure of the Luminescent Aggregates. *J. Phys. Chem. C* **2008**, *112*, 2137−2146.
(31) Hu, R.; Leung, N.-L.-C.; Tang, B.-Z. AIE Macromolecules: Syntheses, Structures and Functionalities. *Chem. Soc. Rev.* **2014**, *43*, 4494−4562.
(32) Ding, D.; Li, K.; Liu, B.; Tang, B.-Z. Bioprobes Based on AIE Fluorogens. *Acc. Chem. Res.* **2013**, *46*, 2441−2453.
(33) Hong, Y.; Lam, J.-W.-Y.; Tang, B.-Z. Aggregation-Induced Emission. *Chem. Soc. Rev.* **2011**, *40*, 5361−5388.
(34) Zhao, Z.; Deng, C.; Chen, S.; Lam, J. W. Y.; Qin, W.; Lu, P.; Wang, Z.; Kwok, H. S.; Ma, Y.; Qiu, H.; Tang, B. Z. Full Emission Color Tuning in Luminogens Constructed from Tetraphenylethene, Benzo-2,1,3-thiadiazole and Thiophene Building Blocks. *Chem. Commun.* **2011**, *47*, 8847−8849.
(35) Shi, J.; Wu, Y.; Sun, S.; Tong, B.; Zhi, J.; Dong, Y. Tunable Fluorescence Conjugated Copolymers Consisting of Tetraphenylethylene and Fluorene Units: From Aggregation-Induced Emission Enhancement to Dual-Channel Fluorescence Response. *J. Polym. Sci., Part A: Polym. Chem.* **2013**, *51*, 229−240.
(36) Aldred, M. P.; Li, C.; Zhang, G.-F.; Gong, W.-L.; Li, A. D. Q.; Dai, Y.; Ma, D.; Zhu, M.-Q. Fluorescence Quenching and Enhancement of Vitrifiable Oligofluorenes End-Capped with Tetraphenylethene. *J. Mater. Chem.* **2012**, *22*, 7515−7528.
(37) Ananthakrishnan, S. J.; Varathan, E.; Ravindran, E.; Somanathan, N.; Subramanian, V.; Mandal, A. B.; Sudha, J. D.; Ramakrishnan, R. A Solution Processable Fluorene−Fluorenone Oligomer with Aggregation Induced Emission Enhancement. *Chem. Commun.* **2013**, *49*, 10742−10744.
(38) Stork, M.; Gaylord, B. S.; Heeger, A. J.; Bazan, G. C. Energy Transfer in Mixtures of Water-Soluble Oligomers: Effect of Charge, Aggregation, and Surfactant Complexation. *Adv. Mater.* **2002**, *14*, 361−366.
(39) Duan, X.; Liu, L.; Feng, F.; Wang, S. Cationic Conjugated Polymers for Optical Detection of DNA Methylation, Lesions, and Single Nucleotide Polymorphisms. *Acc. Chem. Res.* **2010**, *43*, 260−270.
(40) Zhou, J.; Chang, Z.; Jiang, Y.; He, B.; Du, M.; Lu, P.; Hong, Y.; Kwok, H. S.; Qin, A.; Qiu, H.; Zhao, Z.; Tang, B. Z. From Tetraphenylethene to Tetranaphthylethene: Structural Evolution in AIE Luminogen Continues. *Chem. Commun.* **2013**, *49*, 2491−2493.
(41) An, B.-K.; Lee, D.-S.; Lee, J.-S.; Park, Y.-S.; Song, H.-S.; Park, S. Y. Strongly Fluorescent Organogel System Comprising Fibrillar Self-Assembly of a Trifluoromethyl-based Cyanostilbene Derivative. *J. Am. Chem. Soc.* **2004**, *126*, 10232−10233.
(42) Wang, Z.; Chen, S.; Lam, J. W. Y.; Qin, W.; Kwok, R. T. K.; Xie, N.; Hu, Q.; Tang, B. Z. Long-Term Fluorescent Cellular Tracing by the Aggregates of AIE Bioconjugates. *J. Am. Chem. Soc.* **2012**, *135*, 8238−8245.